EurJIC European Journal of Inorganic Chemistry

FULL PAPER

DOI: 10.1002/ejic.201200067

The Reactions of Thianthrene and Selenanthrene with $AlCl_3$: Coordination Complexes, Radical Ions, and Investigations on the Unique Triple-Decker Molecule $(Thianthrene)_3^{2+}$

Rachmat Triandi Tjahjanto,[a][‡] Michael F. Peintinger,[b] Thomas Bredow,[b] and Johannes Beck*[a]

Keywords: Radical ions / Conducting materials / Electron transport / Magnetic properties / Density functional calculations / Sulfur heterocycles / Selenium heterocycles / Aluminum

The reactions of thianthrene (TA) and selenanthrene (SeA) with $AlCl_3$ were studied in the melt phase and with liquid SO_2 as solvent. From neat $AlCl_3$ and TA, the colorless complex $[AlCl_3(TA)]$ was isolated as the main product and the dark red salt $(TA)_3[Al_2Cl_7]_2$ as the byproduct. The analogous solvent-free reaction of selenanthrene and $AlCl_3$ takes a different course as colorless $[Al(SeA)_3][Al_2Cl_7]_3$ is formed in quantitative yield. With SO_2 as solvent, both TA and SeA give the black radical salts $(TA)_2[AlCl_4]_2$ and $(SeA)_2[AlCl_4]_2$, respectively. In the structure of $[AlCl_3(TA)]$, thianthrene acts as a monodentate ligand and coordinates with one S atom to the pyramidal $AlCl_3$ unit. The structure of the $(TA)_3^{2+}$ ion is a stack of three almost planar TA molecules in parallel arrangement. $[Al(SeA)_3]^{3+}$ represents a tris-chelate complex ion with SeA acting as a bidentate ligand and both Se atoms binding to the octahedrally coordinated Al^{3+} ion. $(SeA)_2[AlCl_4]_2$ consists of dimers of SeA^+ radical ions, which are bound by weak intermolecular Se···Se bonds. Tentative reaction equations are given to explain the unexpected oxidation processes that lead to the radical ions. Quantum chemical calculations were performed on the molecular fragments and on the periodical structures. The trimeric $(TA)_3^{2+}$ ion is in the singlet state in accordance with the magnetic properties of $(TA)_3[Al_2Cl_7]_2$, which show a weak temperature-independent paramagnetism. The ion is bound by long-range four-center bonds between the outer two radicals.

Introduction

The development of conductive molecular materials has been the focus of research for several decades. The assembly of radical molecules in the crystal is one of the main synthetic approaches.[1] Organic radicals are in most cases highly reactive and short-lived intermediates. Electron delocalization over a π-electron system within the molecule and the presence of heavier atoms enhance the stability and can lead to stable, persistent radicals. Sulfur atoms play a predominant role in the stabilization. In sulfur-bearing aromatic compounds, the sulfur lone pairs are close in energy to the carbon π orbitals and contribute to the presence of an electron-rich system.

Materials with the desired properties can be obtained in different ways. Numerous charge-transfer salts based on charged, planar-shaped organic radicals have been synthesized. Tetrathiafulvalenium (TTF) radical cations and tetracyanoquinodimethanide (TCNQ) radical anions are the most widely used. The use of neutral radical molecules is a newer and promising approach because electrostatic repulsions, always present between cationic or between anionic radical ions, do not need to be overcome for an effective intermolecular orbital overlap. Dithiazolyl radicals turned out to be suitable building units, since a low dimerization enthalpy is present.[2] Recently it was shown that the application of moderate pressure is able to transform bisthiaselenazolyl radicals from a semiconducting to a metallic material.[3]

Thianthrene (TA), a sulfur-bearing heterocyclic molecule, allows for reversible electron-transfer reactions. Since the very beginning of its chemistry in the nineteenth century, thianthrene has been known to form a persistent radical cation. Originally observed by the intensive purple color of the solution in concentrated sulfuric acid, the $(TA)^{\cdot+}$ radical cation is today a well-known species. Due to the stability of the respective solid salts, $(TA)^{\cdot+}$ has gained a relevance in radical-ion chemistry and is used as a specific one-electron oxidant.[4] Several ways for the one-step oxidation of TA to the radical cation have been reported, among them the reaction of TA with $NO[BF_4]$[5] or the reaction of TA with $AlCl_3$ in dichloromethane.[6] Structural determinations of the thianthrene radical-ion tetrachloridoaluminate[6] and hexafluoridophosphate[7] revealed the significant structural change caused by the oxidation. In contrast to the neutral

[a] Institute for Inorganic Chemistry, University of Bonn, Gerhard-Domagk-Strasse 1, 53121 Bonn, Germany
E-mail: j.beck@uni-bonn.de
[b] Mulliken Center for Theoretical Chemistry, Institute für Physical and Theoretical Chemistry, University of Bonn, Beringstrasse 4, 53115 Bonn, Germany
[‡] Current address: Universitas Brawijaya Chemistry Department, Malang, Indonesia

molecule, which in the crystal is bent along the intramolecular S···S axis with an interplanar angle between the two $C_6H_4S_2$ groups of 128°,[8] the radical ions in $(TA^{\cdot+})X^-$ (X^- = $[AlCl_4]^-$, $[PF_6]^-$) are almost planar and form pairs $(TA)_2^{2+}$ with weak intermolecular S···S bonds and ecliptic configuration in the solid state {S···S 3.08 Å for $(TA)_2[AlCl_4]_2$, 3.06 Å for $(TA)_2[PF_6]_2$} (Scheme 1).

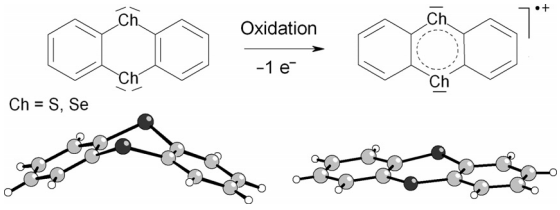

Scheme 1. The one-electron oxidation of thianthrene (TA) and selenthrene (SeA) to the respective radical cations is accompanied by a conformational change. The bent neutral molecules with dihedral angles along the Ch···Ch axis (128° for TA, 127° for SeA) are flattened upon formation of the respective radical cations.

A surprising result was recently reported by the one-electron oxidation of TA with the dodecamethylcarbaboranyl radical in hexane/CH_2Cl_2 to yield $(TA)_3[B_{11}C(CH_3)_{12}]_2$.[9] In the crystal structure, the $(TA)_3^{2+}$ ion is present, which consists of a stack of three TA moieties in parallel arrangement of the molecular planes. The central, planar molecule is twisted by 90° against the two outer slightly bent molecules, thus giving the trimer approximately D_{2h} symmetry. Since the intramolecular S···S axes of the three individual TA units are perpendicular to each other, there is no direct intermolecular S···S interaction between the molecules, which stands in sharp contrast to the cofacial radical-ion dimers $(TA)_2^{2+}$. A theoretical consideration showed, however, that the interactions of the partially occupied HOMOs allow for a bonding combination even for molecules in perpendicular arrangement.[9]

The free electron pairs on the sulfur atoms allow TA to act as a complex ligand and several metal complexes with the butterfly-shaped molecule are known. TA can act as a monodentate ligand by coordination through one of the sulfur atoms, as found for $[AuCl_3(TA)]$[10] or $[AuCl_2(TA)_2][AuCl_4]$.[11] The bidentate coordination mode is observed in positively charged silver complexes with weakly coordinating anions, as present in the structures of $[Ag(ClO_4)(TA)]_2$,[12] $[Ag_2(TA)_3][SbF_6]_2 \cdot 5SO_2$, and $[Ag_2(TA)_2][BF_4]_2 \cdot 3SO_2$.[13] When TA acts as ligand, no large changes in the molecular structure are observed, in considerable contrast to the flattening of the molecule on oxidation.

Selenanthrene (SeA) is generally less explored than thianthrene. Analogous to TA, the molecule is bent in the crystal by 127°[14] and is known to undergo a one-electron oxidation to the radical cation and a second oxidation step to the dication.[15,16] The electron-donor properties of SeA have been proven by the formation of a charge-transfer complex with TCNQ.[17]

The formation of radicals, detectable by EPR spectroscopy, upon mixing various heteroaromatic compounds with aluminum chloride is a known effect, in particular for thianthrene. Heating TA with anhydrous aluminum chloride without solvent to temperatures between 60 and 180 °C and cooling to room temperature was reported to give a deeply colored solid that has no paramagnetism.[18] The coloration, however, implies the formation of oxidized forms of thianthrene. The mechanism and the emerging chemical species remained unclear.

Despite the fact that these observations were made decades ago, no thorough chemical study on the remarkable solvent-free reaction between TA and aluminum chloride has been performed to the best of our knowledge. The intention of the present work is to give a deeper insight to this reaction, which we expanded to include selenanthrene and the weakly coordinating solvent liquid sulfur dioxide.

Results and Discussion

The Reactions of Thianthrene and Selenanthrene with $AlCl_3$

Mixing TA with $AlCl_3$ at ambient temperature under strictly dry and anaerobic conditions immediately effects a bluish-violet coloration of both colorless starting materials. Heating to 150 °C for 12 h converts the mixture to a dark blue, viscous melt. Annealing at 50 °C in a slight temperature gradient causes the sublimation of large, transparent, strongly light-refracting crystals of $[AlCl_3(TA)]$, which is the main product. During prolonged annealing, and commencing after some days, the formation of additional phases was observed. In small amounts, dark red, transparent crystals with the shape of flat needles deposited mainly in the zone at around 40 °C, which were analyzed as $(TA)_3[Al_2Cl_7]_2$ that contained the oxidized thianthrene species $(TA)_3^{2+}$. It could be observed that these crystals grew in the blue melt drops until the blue color faded away, thus leaving the dark crystals embedded in colorless drops. The yield was very small in all runs and did not exceed 10%. An even smaller amount of yellow, transparent, platelike crystals was observed in all runs. Unfortunately, we did not succeed in their characterization. The yellow crystals grew as thin plates and strongly adhered to the glass walls; they were very soft and mechanically sensitive and could not be separated without being destroyed. The gas phase plays an important role in the reaction. If the amount of reactants was too small for a given reaction vessel volume, the yields of the colored products diminished strongly.

With selenanthrene (SeA), the reaction with neat $AlCl_3$ takes a completely different course. Blue colorations, typical for the reaction with TA, were not observed. Instead, in closed ampoules at 90 °C colorless crystals of $[Al(SeA)_3][Al_2Cl_7]_3$ were obtained. Using SeA and $AlCl_3$ in 3:7 stoichiometric ratio gave $[Al(SeA)_3][Al_2Cl_7]_3$ in quantitative yield. The reaction follows the straightforward Equation (1).

$$3SeA + 7AlCl_3 \rightarrow [Al(SeA)_3][Al_2Cl_7]_3 \quad (1)$$

The reaction is unique and remarkable. Formally, one $AlCl_3$ molecule releases all three Cl^- ions and acts as a

Lewis base. Six $AlCl_3$ molecules act as Lewis acids and take up the chloride ions, thereby forming three dinuclear $[Al_2Cl_7]^-$ ions. Al^{3+} is coordinated by three SeA molecules as bidentate ligands to form the complex cation $[Al(SeA)_3]^{3+}$. Oxidation of SeA does not occur under these conditions. After prolonged heating for several weeks, the crystals turned grayish, which on microscopic inspection turned out to be a covering of the transparent crystals by a thin layer of violet oil. This shows that not only the Lewis acid–base reaction takes place, but to a lower extent and at much slower reaction rate the formation of oxidized species as observed for thianthrene occurs, for which this is the predominant reaction. The different behavior of TA and SeA is surprising, since the oxidation potentials of the first two oxidation steps are similar (SeA: E_1 = +0.85, E_2 = +1.44 V; TA: E_1 = +0.91, E_2 = +1.26 V, both in acetonitrile against $Ag/AgNO_3$).[15]

The course of the reactions of TA and SeA with $AlCl_3$ changes completely if carried out in liquid SO_2 as solvent. At ambient temperature, $AlCl_3$, thianthrene, and selenanthrene are all thoroughly soluble, with the latter two giving yellow solutions, whereas the solution of $AlCl_3$ is colorless. After combining solutions of TA and $AlCl_3$ or SeA and $AlCl_3$, dark blue colorations emerged instantaneously and black crystals with metallic luster started to precipitate within minutes. These were identified as the respective radical cation chloridoaluminates $(TA)_2[AlCl_4]_2$ and $(SeA)_2[AlCl_4]_2$. Crystals of $(TA)_2[AlCl_4]_2$ were identified by their lattice constants[6] and a crystal structure determination of the yet unknown $(SeA)_2[AlCl_4]_2$ was carried out (vide infra).

The reaction between TA and aluminum chloride is only partly understood. $AlCl_3$ in CH_2Cl_2 is known to be a strong oxidizing agent for which an oxidation potential of 1.6 V has been assigned.[19] To understand the high oxidizing power of this reaction system, it may be assumed that $(CH_2Cl)^+[AlCl_4]^-$ is formed as an intermediate with the carbenium ion as the oxidizing species, which itself is finally reduced to ClH_2CCH_2Cl. However, the presence of such oxidizing intermediates cannot be assumed with neat $AlCl_3$ nor with $AlCl_3/SO_2$, and the question of the nature of the oxidizing species remains open.

We examined both kinds of reactions, the first one without solvent and the second one by using liquid SO_2, to gain insight to the mechanisms. When the reaction ampoules that contained TA and neat $AlCl_3$—which contained the blue solidified melt and dark red crystals of $(TA)_3[Al_2Cl_7]_2$, thereby indicating that the redox process had occurred—were broken and wrapped with wet lead acetate paper, a black coloration effected by the precipitation of PbS was observed within a few minutes. The slow process indicates that a hydrolyzable sulfide compound had formed, which forms H_2S upon contact with moist air. As a consequence, one can assume that the oxidation process proceeds through desulfuration of thianthrene to dibenzothiophene (DBTh, $C_{12}H_8S$) accompanied by the formation of aluminum sulfide chloride AlSCl according to the tentative reaction Equation (2).

$$5TA + 6AlCl_3 \rightarrow (TA)_3[Al_2Cl_7]_2 + [AlCl_3(TA)] + AlSCl + C_{12}H_8S \quad (2)$$

Attempts to detect DBTh by means of mass spectrometry were inconclusive. The analysis of the dark blue mass revealed a signal at *m*/*z* 184. This signal is also predominantly present in the mass spectrum of pure TA, which represents the most common fragmentation process. In the blue $TA/AlCl_3$ reaction mass, however, this signal appeared with 10% higher relative intensity than in the spectrum of neat thianthrene.

When the reaction between TA and $AlCl_3$ is performed in liquid SO_2 as solvent, the radical salt $(TA)_2[AlCl_4]_2$ is the major product and is formed even at low temperatures and in a very short time. To rule out the possibility that impurities of SO_3 in commercial SO_2 were responsible for the oxidation, we synthesized SO_2 from H_3PO_4 and $NaHSO_3$ to exclude the presence of any SO_3 (see the Experimental Section). In the solvent prepared in this way, the reaction between TA and $AlCl_3$ gave the same result as in commercial SO_2. It is clear that SO_2 takes part in the reaction. One can assume that it acts as an oxidant and is reduced to the radical ion $(SO_2)^{\cdot-}$, which dimerizes to dithionite $S_2O_4^{2-}$. The overall reaction can be formulated according to the tentative reaction Equation (3).

$$6TA + 8AlCl_3 + 6SO_2 \rightarrow 3(TA)_2[AlCl_4]_2 + Al_2(S_2O_4)_3 \quad (3)$$

According to this equation, one expects a specific weight increase in the reaction products due to the uptake of solvent. That SO_2 is actually involved in the reaction was shown by gravimetric analyses of different runs. If TA was used in an excess amount and the amount of $AlCl_3$ was made the limiting factor, a constant increase in the weight of the reaction products was found after exhaustive pumping off of all volatiles. The increase amounted to 0.74(2) molar equivalents SO_2 for each mole of $AlCl_3$ according to a ratio of 3 mol SO_2 to 4 mol $AlCl_3$, which is in line with Equation (3). The Raman spectra of the aqueous extract showed mainly broad signals (400, 1100, 1600 cm^{-1}), which coincide but could not be unequivocally assigned to the typical bands for dithionite.[20] The qualitative test for dithionite through the decomposition of hydroxymethylsulfinate (Rongalite) to H_2S,[21] however, gave no positive result.

Crystal Structures

Trichlorido(thianthrene)aluminum(III) [$AlCl_3$(TA)]

The asymmetric unit consists of two independent molecular complexes (Figure 1; in the following discussion named complex **1** and complex **2** for the complexes that contain Al1 and Al2, respectively). The thianthrene molecule in each complex is coordinated to the Al atom through one of the S atoms, thus acting as a monodentate ligand. The aluminum atoms gain a distorted tetrahedral coordination. As expected, the Al–S bonds (average 2.40 Å) are substantially longer than the Al–Cl bonds (average 2.10 Å), and the S–Al–Cl angles (average 103.5°) are smaller than the Cl–

Al–Cl angles (average 114.6°). This mode of coordination is similar to that of $[AuCl_3(TA)]$,[10] in which, however, the metal ion is in square-planar coordination, typical for trivalent gold.

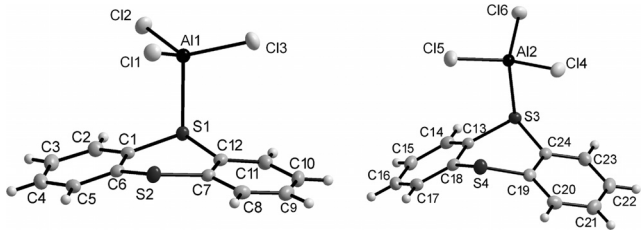

Figure 1. The two crystallographically independent molecules in the structure of $[AlCl_3(TA)]$. Thermal ellipsoids are scaled to include a probability density of 50%. Selected bond lengths [Å] and angles [°]: Al1–S1 2.3804(9), Al1–Cl1 2.1031(9), Al1–Cl2 2.1058(9), Al1–Cl3 2.1011(9), S1–C1 1.781(2), S1–C12 1.781(2), S2–C6 1.763(2), S2–C7 1.756(2), Al2–S3 2.4219(9), Al2–Cl4 2.1115(9), Al2–Cl5 2.1015(9), Al2–Cl6 2.1048(9), S3–C13 1.781(2), S3–C24 1.785(2), S4–C18 1.769(2), S4–C19 1.765(2), C–C within phenyl rings 1.378(4) to 1.398(3); S1–Al1–Cl1 106.99(4), S1–Al1–Cl2 101.61(4), S1–Al1–Cl3 101.70(4), Cl1–Al1–Cl2 112.43(4), Cl1–Al1–Cl3 115.07(5), Cl2–Al1–Cl3 116.86(4), S3–Al2–Cl4 100.73(3), S3–Al2–Cl5 110.09(4), S3–Al2–Cl6 100.19(4), Cl4–Al2–Cl5 118.76(4), Cl4–Al2–Cl6 111.71(4), Cl5–Al2–Cl6 112.94(4).

The key differences between the two independent complexes lie in the dihedral angles of the attached TA molecules and in the rotational conformation of the $AlCl_3$ groups with respect to the TA ligand. In complex **1**, the dihedral angle between the two $C_6H_4S_2$ moieties of the TA molecule amounts to 156.0°, whereas the respective angle in complex 2 is 130.2°, which corresponds to the value found for neat TA in the crystal. Different conformations are present for the two complexes with respect to the rotation of the $AlCl_3$ group around the Al–S axis. In complex **1**, the $AlCl_3$ group is oriented in such a way that atom Cl1 is located over the centroid of the central ring S1–C1–C6–S2–C7–C12 of the TA ligand. The S2····S1–Al1 angle amounts to 95.1°, thus bringing the $AlCl_3$ group in an *exo* position with respect to the TA ligand. In complex **2**, the $AlCl_3$ group is oriented differently. The bonds Al2–Cl4 and Al2–Cl5 are coincident with the bonds S3–C13 and S3–C24 in the view along the Al2–S3 axis. A short Cl4···C24 contact of 3.38 Å is present, which is slightly shorter than the sum of the van der Waals radii (3.45 Å). The stronger bending of the TA ligand in complex **2** may thus be attributed to steric repulsion. The S4····S3–Al2 angle amounts only to 83.2°, thereby indicating the *endo* position for the $AlCl_3$ group.

Tris(thianthrene)–Bis(heptachloridodialuminate) $(TA)_3[Al_2Cl_7]_2$

The crystal structure consists of stacks composed of three flattened TA molecules in an ecliptic arrangement and heptachloridodialuminate ions (Figure 2). For each of the $(TA)_3$ stacks there are two $[Al_2Cl_7]^-$ ions present, which allows the unambiguous assignment of the ionic charge $(TA_3)^{2+}$. An inversion center is located in the center of gravity of the TA molecule in the middle of the stack. The central molecule is essentially planar. The largest deviation of all 22 atoms from the least-squares plane amounts to 0.02 Å. The peripheral TA molecules are symmetry related by the inversion center and slightly bent along the S···S axis with a dihedral angle of 164.1°. The average lengths of the four S···S contacts between the three TA molecules amounts to 3.167 Å, which is 0.1 Å longer than that found in the $(TA)_2^{2+}$ dimers of two radical cations. The $(TA_3)^{2+}$ trimer possesses only C_i symmetry in the crystal, but the higher point symmetry D_{2h} is almost fulfilled.

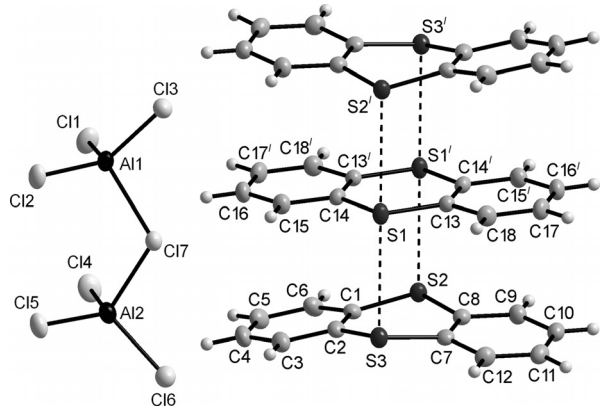

Figure 2. The molecules $(TA)_3^{2+}$ and $[Al_2Cl_7]^-$ in the structure of $(TA)_3[Al_2Cl_7]_2$. Thermal ellipsoids are scaled to include a probability density of 50%. Symmetry operation: $1-x$, $1-y$, $1-z$. Selected bond lengths [Å] and angles [°]: S1–C13 1.729(2), S1–C14 1.732(2), S2–C1 1.746(2), S2–C8 1.747(2), S3–C2 1.745(2), S3–C7 1.742(2), S1···S3 3.1587(9), S1···S2^I 3.1747(9), Al1–Cl1 2.1030(8), Al1–Cl2 2.1083(8), Al1–Cl3 2.1023(9), Al2–Cl4 2.0990(9), Al2–Cl5 2.1089(9), Al2–Cl6 2.1088(9), Al1–Cl7 2.2836(9), Al2–Cl7 2.2872(9), C–C within phenyl rings 1.372(3) to 1.411(3); S3–S1–S2^I 179.74(3), C13–S1–C14 107.5(1), C1–S2–C8 106.4(1), C2–S3–C7 106.3(1), Al1–Cl7–Al2 114.75(3).

The S–C bond lengths in thianthrene molecules depend characteristically on the oxidation state. In the neutral form the S–C bond lengths are on average 1.77 Å. In the oxidized form, these bonds are shortened to 1.73 Å as found in the crystal structures of $(TA)_2[AlCl_4]_2$[6] and $(TA)_2[PF_6]_2$.[7] The TA molecule in the middle of the $(TA_3)^{2+}$ stack has average S–C bond lengths of 1.730 Å, coincident with the radical form. The two peripheral molecules exhibit S–C bonds of 1.745 Å, longer than in the radical cation but shorter than in the neutral form. These bond lengths indicate the dispersion of the positive charges over the entire trimer with a maximum of the charge on the central molecule.

The dinuclear anion $[Al_2Cl_7]^-$ is a well-known species and is generally formed from $[AlCl_4]^-$ and $AlCl_3$ in the presence of large cations. In the crystal structure of $(TA)_3[Al_2Cl_7]_2$ the anion has no crystallographic symmetry but the configuration is only slightly distorted from C_{2v}. All terminal Cl atoms have short bonds to the Al atoms (average 2.105 Å) relative to the bridging Cl atom (average 2.285 Å). The overall shape is a corner-sharing pair of two distorted tetrahedra $[Cl_3Al–Cl–AlCl_3]^-$.

In the crystal, the $(TA_3)^{2+}$ cations are isolated from each other and no extended stacking is observed. There are six $[Al_2Cl_7]^-$ anions that surround each cation in one plane

with their Al···Al axes parallel to the $(TA)_3$ stacking direction (Figure 3). On account of the large monoclinic angle of close to 120°, these $(TA)_3[Al_2Cl_7]_6$ groups are shifted against each other parallel to the crystallographic *b*–*c* plane, which completes the coordination sphere of each $(TA)_3$ group to eight coordinating anions in the form of a bicapped hexagonal prism.

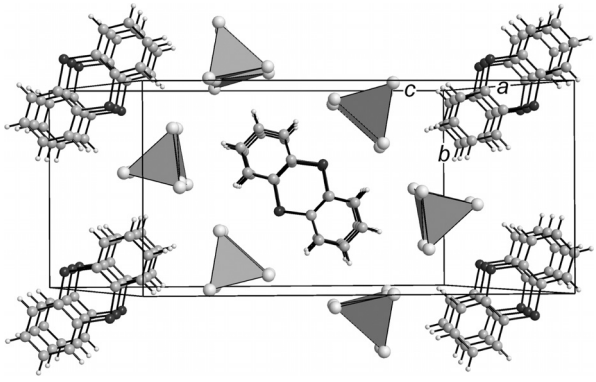

Figure 3. The unit cell of the crystal structure of $(TA)_3[Al_2Cl_7]_2$ in a perspective view along the $(TA)_3$ stacks. All atoms are drawn with spheres of arbitrary radii. The $[Al_2Cl_7]^-$ ions are represented as connected tetrahedra.

Tris(selenanthrene)aluminum–Tris(heptachloridodialuminate) $[Al(SeA)_3][Al_2Cl_7]_3$

The asymmetric unit of the monoclinic cell contains one cationic complex $[Al(SeA)_3]^{3+}$ and three independent $[Al_2Cl_7]^-$ anions (Figure 4, Table 3). In the cationic complexes, three SeA molecules coordinate the Al central atom each as a bidentate ligand. The coordination environment of the Al atom is a slightly distorted octahedron. The six Al–Se bond lengths are almost equal with an average of 2.593 Å; they differ only by 0.01 Å. The deviation from ideal octahedral symmetry arises from the ligand bite of the SeA molecules. The Se–Al–Se angles of the coordinating Se atoms that belong to the same SeA molecule amount to 78.5° on average. The coordinated SeA molecules show a

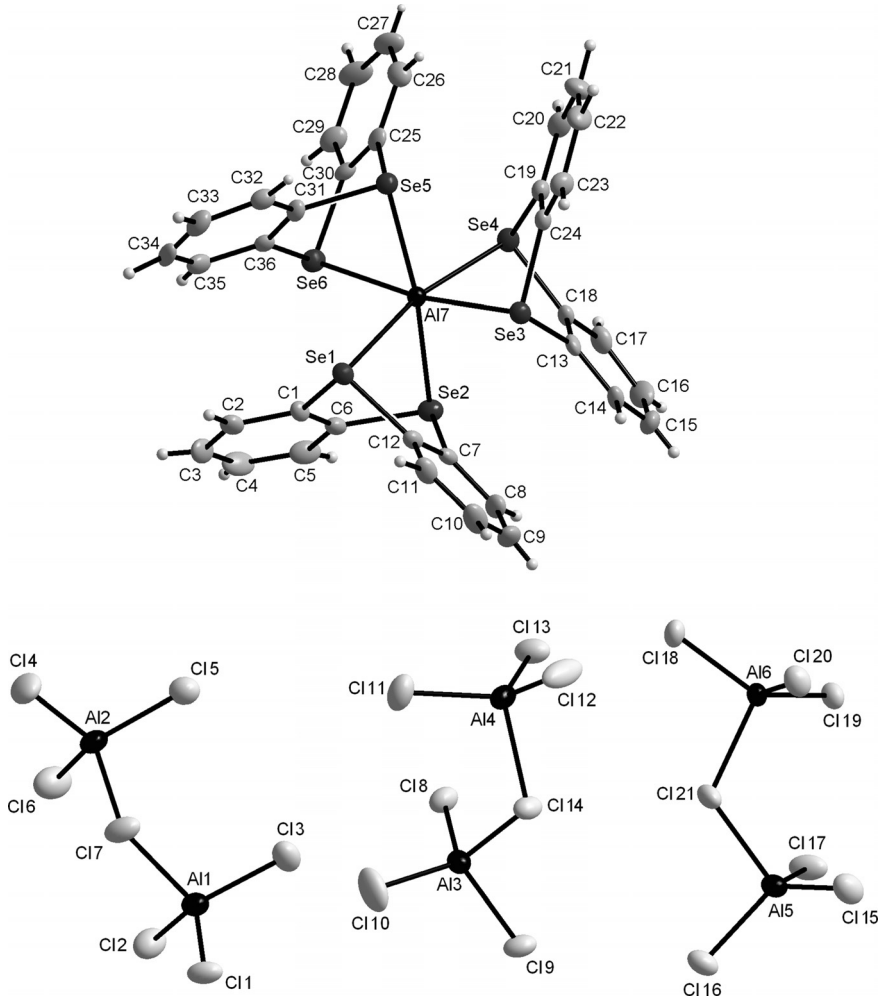

Figure 4. The complex cation $[Al(SeA)_3]^{2+}$ and the three independent $[Al_2Cl_7]^-$ anions in the structure of $[Al(SeA)_3][Al_2Cl_7]_3$. Thermal ellipsoids are scaled to include a probability density of 50%. Selected bond lengths [Å] and angles [°]: Al7–Se 2.588(2) to 2.598(2), Se–C 1.909(5) to 1.931(5), C–C within phenyl rings 1.364(8) to 1.402(7), Al–$Cl_{terminal}$ 2.088(2) to 2.127(2), Al–$Cl_{bridging}$ 2.257(2) to 2.291(2); Se1–Al7–Se2 78.39(4), Se3–Al7–Se4 78.91(4), Se5–Al7–Se6 78.40(4), all other *cis* Se–Al7–Se 90.71(5) to 98.66(5), *trans* Se–Al7–Se 168.01(6) to 172.48(6), C–Se–C 90.6(2) to 96.8(2), Al1–Cl7–Al2 116.37(9), Al3–Cl14–Al4 114.18(8), Al5–Cl21–Al6 118.10(8).

folding along the Se···Se axis of 117.0, 118.5, and 120.0°, slightly lower than observed in the uncomplexated state. The $[Al(SeA)_3]^{3+}$ molecules have no crystallographic symmetry but are close to the symmetry of point group D_3, which is the typical molecular symmetry for tris(chelate) complexes. The individual complexes are chiral, but the centrosymmetry of the crystal lattice causes both enantiomorphs to be present, thus making the crystals racemic. The structural parameters of the heptachloridodialuminate ions are analogous to the respective anions in the structure of $(TA)_3[Al_2Cl_7]_2$ and show no peculiarities.

In the crystal, the cationic complexes gain a high coordination number by surrounding $[Al_2Cl_7]^-$ anions. Each $[Al(SeA)_3]^{3+}$ complex is surrounded by 14 anions in a strongly distorted hexacapped cubic arrangement. This coordination provides an effective way to shield the high charge of the cations by the weakly coordinating and low-charged anions.

Selenanthrene–Tetrachloridoaluminate $(SeA)_2[AlCl_4]_2$

$(SeA)_2[AlCl_4]_2$ crystallizes isotypic to the sulfur-bearing analogue $(TA)_2[AlCl_4]_2$[3] in the orthorhombic space group $P2_12_12_1$. With respect to $(TA)_2[AlCl_4]_2$, the unit-cell volume of $(SeA)_2[AlCl_4]_2$ is enlarged by 110 Å^3 or by 3.5%. The structure contains pairs of selenanthrene radical cations $(SeA^{\cdot+})_2$ and tetrahedral $[AlCl_4]^-$ ions (Figure 5). The $(SeA^{\cdot+})_2$ dimers do not possess crystallographic symmetry, but are close to C_{2v} point symmetry. Each two selenanthrene radical ions are arranged in parallel fashion and held together by Se···Se bonds with average lengths of 3.15 Å. The two individual SeA radicals are almost but not completely flat. The dihedral angles of the $C_6H_4Se_2$ moieties amount to 172.3° for molecule **1** and 173.6° for molecule **2**. The two ions are slightly shifted with respect to each other with the consequence that the four Se atoms of each dimer do not form a rectangular, but a rhomboidal arrangement. The confacial arrangement of the two almost planar radical ions leads to the interpretation of the $(SeA^{\cdot+})_2$ ion as a π dimer in analogy to $(TA^{\cdot+})_2$.[22]

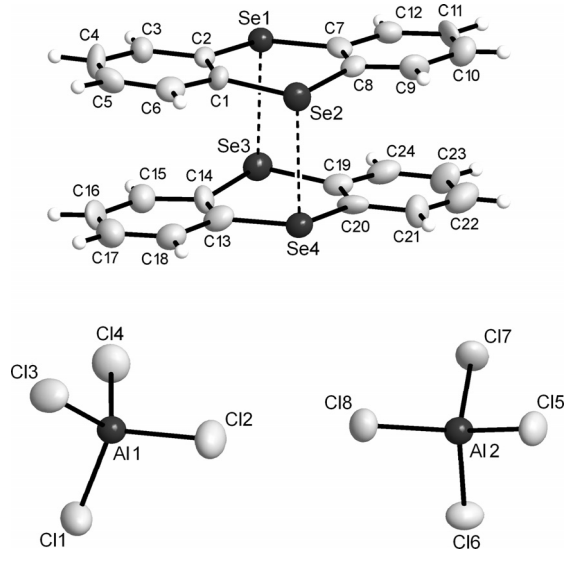

Figure 5. The molecules in the structure of $(SeA)_2[AlCl_4]_2$. Thermal ellipsoids are scaled to include a probability density of 50%. Selected bond lengths [Å] and angles [°]: Se1–C2 1.866(9), Se1–C7 1.88(1), Se2–C1 1.87(1), Se2–C8 1.865(9), Se3–C14 1.86(1), Se3–C19 1.87(1), Se4–C13 1.89(1), Se–C20 1.88(1), Se1···Se3 3.132(1), Se2···Se4 3.182(1), Al–Cl 2.110(4) to 2.134(4), C–C within phenyl rings 1.35(2) to 1.43(2); C–Se–C 104.8(5) to 106.0(4), Cl–Al–Cl 107.4(2) to 110.9(2).

Magnetic Properties of $(TA)_3[Al_2Cl_7]_2$

The magnetic properties of $(TA)_3[Al_2Cl_7]_2$ have been investigated in the temperature range of 20–300 K. In the interval 50–250 K, a small paramagnetic moment between 5×10^{-4} and 1×10^{-3} cm^3 mol^{-1} was observed. In this region, the susceptibility is almost unaffected by the temperature but dependent on the applied field. Below 50 K the moment decreases and reaches 3×10^{-4} cm^3 mol^{-1} at 20 K. The magnetic properties of $(TA)_3[Al_2Cl_7]_2$ are thus best described as a temperature-independent paramagnetism (TIP).

Quantum Chemical Calculations

To analyze the electronic structure and bonding situation of the thianthrenes and selenanthrenes, quantum chemical calculations of the corresponding bulk structures and of representative molecular fragments were performed.

Firstly, the geometries and electronic structures of the thianthrene radical cation $(TA)^{\cdot+}$ and the selenanthrene radical cation $(SeA)^{\cdot+}$ were calculated in the gas phase at the DFT level. The singly occupied molecular orbital (SOMO, B_{1u} symmetry) of $(TA)^{\cdot+}$ is shown in Figure 6 (a). The SOMO of the isoelectronic $(SeA)^{\cdot+}$ has a very similar shape. In both radicals, the unpaired electron is mainly delocalized over the central heterocyclic ring. In the radical

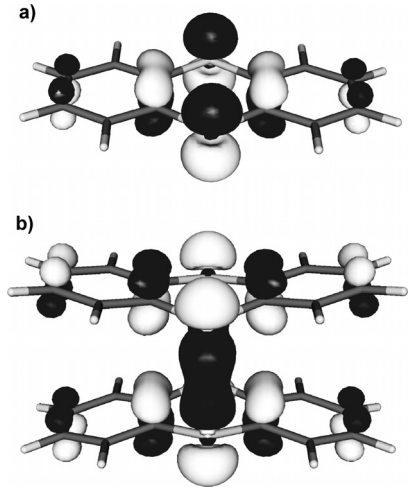

Figure 6. (a) The SOMO of the thianthrene radical cation $(TA)^{\cdot+}$ calculated (PBE0/def2-TZVPP) in the gas phase. The spin density is primarily delocalized in the central heterocyclic ring. The SOMO of the valence isoelectronic selenanthrene radical cation $(SeA)^{\cdot+}$ is of almost identical shape. (b) The bonding MO (A_g symmetry) of the $(TA_2)^{2+}$ dimer formed out of the two SOMOs of thianthrene radical cations $(TA)^{\cdot+}$ calculated at the PBE0–D3/def2-TZVPP level in the gas phase.

dimer $(TA)_2^{2+}$ a four-center, two-electron bond is formed between the sulfur atoms. The bonding MO (A_g symmetry) is formed out of the two SOMOs of the radical monomers (Figure 6, b).

Periodic quantum chemical calculations were performed to study the electronic structure of $[AlCl_3(TA)]$, $(TA)_3[Al_2Cl_7]_2$, $[Al(SeA)_3][Al_2Cl_7]_3$, and $(SeA)_2[AlCl_4]_2$. The PBE exchange-correlation functional of Perdew, Burke, and Ernzerhof[23,24] that represents one of the de facto standard methods in solid-state quantum chemistry was employed. We used our recently developed pob-TZVP solid-state basis sets.[25] As a first step, full structure optimizations of all atom positions were performed in different electronic states. The lattice parameters were kept fixed at their experimental values. As it is well known that standard density functional theory does not account for dispersion effects that might be expected to have an effect on the intermolecular interaction between the TA or SeA molecules, we employed an empirical correction scheme,[26] as implemented in CRYSTAL09,[27] indicated by PBE-D2. In gas-phase calculations of cluster models the more recent D3 version of the dispersion correction[28] as implemented in the ORCA program system[29] was employed. Here we employed standard def2-TZVPP basis sets.[30,31] It is well known that the Hartree–Fock method overly stabilizes high-spin states, whereas GGA DFT methods tend towards spin pairing due to the self-interaction error.[32] It was previously[33,34] shown that for the study of electronic and thermodynamic properties of oxides and other compounds, hybrid Hartree–Fock methods give better results than standard DFT methods. We therefore chose the hybrid method PBE0[35] as a more reliable approach for single-point and band structure calculations. The exchange functional is a mixture of 25% HF and 75% PBE.

Trichloridothianthrene Aluminum(III) [$AlCl_3$(TA)]

The primitive unit cell contains four formula units. Structure optimizations were performed for singlet and triplet states to account for possible spin-unpaired situations. PBE predicts the singlet state to be more stable by 2.9 eV than the triplet state. With PBE0 (single-point energies at the optimized PBE structure) the singlet state is even 3.9 eV more stable than the triplet state. Selected structural parameters of the singlet state are given in Table 1; for atom numbering, see Figure 1. In general, the calculated interatomic distances are in reasonable agreement with the experiment with deviations smaller than 0.04 Å for bond lengths and 2.7° for angles. The bending angle of the TA ligand (calculated as the dihedral angle C2–S1–S2–C8) is very close to the experimental value. The valence and conduction bands of singlet $[AlCl_3(TA)]$ are rather flat. The fundamental band gap is 5 eV, thereby classifying $[AlCl_3(TA)]$ as an insulator. To analyze the effect of the rotational conformation of the $AlCl_3$ groups with respect to the TA ligand (vide supra), optimizations of complex **1** and complex **2** were performed in the gas phase as free clusters. The difference of the total energy between the two complexes is small ($\Delta E_{1,2}$ = –0.4 kJ mol^{-1}) and lies within the error range of the method. We therefore conclude that packing effects are responsible for the observed conformations in the solid state.

Table 1. Selected experimental and calculated structure parameters (lengths in Å, angles in °) for $[AlCl_3(TA)]$. For atom numbering, see Figure 1.

Method	Singlet electronic state		
	Exp.	PBE	PBE-D2
	$[AlCl_3(TA)]$ (complex **1**)		
S1–Al1	2.380(1)	2.414	2.405
S1···S2	3.420(1)	3.464	3.476
S2···S1–Al1	95.12(4)	93.4	93.2
S2–S1–Al1–Cl1	12.56(5)	11.6	10.2
α (C2–S1–S2–C8)	156.94(8)	158.9	157.8
	$[AlCl_3(TA)]$ (complex **2**)		
S3–Al2	2.422(1)	2.459	2.445
S3···S4	3.221(1)	3.216	3.238
S4···S3–Al2	83.21(4)	78.3	78.5
S4–S3–Al2–Cl5	51.18(6)	53.7	50.2
α (C14–S3–S4–C20)	128.97(7)	130.1	129.0

Tris(thianthrene)–Bis(heptachloridodialuminate) $(TA)_3[Al_2Cl_7]_2$

The primitive unit cell contains two formula units. Structure optimizations were performed for the unit cell in the closed-shell singlet and open-shell quintet state, the latter assuming both $(TA)_3^{2+}$ units in triplet states. PBE and PBE0 both favor the singlet state, by 1.0 and 0.6 eV, respectively, per cell. From these results, we conclude that the ground state is a singlet state. This is in agreement with the magnetic measurements that showed a TIP, which is due to spin–orbit coupling and not to the presence of unpaired electrons. The calculated structural properties of the singlet state are given in Table 2, in which they are compared to the measured values reported earlier in this study. The values of α_1 and α_2 correspond to the average bending angles of the outer TA molecules (see Figure 2). The experimental structure is thoroughly reproduced in the singlet state, thus indicating that this is indeed the ground state. The effect of dispersion on the $(TA)_3$ substructure is small. Whereas the average S···S distances between the two neighboring TA molecules are slightly improved by the D2 correction, the average dihedral angle α is, however, overestimated.

Table 2. Selected calculated structure parameters (lengths in Å, angles in °) of $(TA)_3[Al_2Cl_7]_2$ and comparison with experimental values. For atom numbering, see Figure 2.

Method	Singlet electronic state		
	Exp.	PBE	PBE-D2
S2′···S1	3.175(2)	3.195	3.181
S1···S3	3.159(2)	3.247	3.233
S···S avg.	3.167	3.221	3.207
α_1 (C6–S2–S3–C12)	160.98(7)	168.5	169.4
α_2 (C3–S3–S2–C9)	165.08(7)	163.9	166.3
C1–C2–C7–C8	2.6(2)	2.9	1.9

In the following we discuss the band structure only for the singlet state. At the PBE0 level the maximum of the valence band (VB) and the minimum of the conduction

band (CB) coincide at the B point (<0.5,0,0> in the conventional setting) of the irreducible Brillouin zone. The direct transition energy is 0.9 eV, thus classifying $(TA_3)[Al_2Cl_7]_2$ as a small-band-gap semiconductor. The small band gap is also in qualitative agreement with the observed dark red color. Kochi et al.[9] presented the first compound that featured $(TA)_3^{2+}$ units. In this so-called "crossed trimer," the central molecule is rotated by 90° around the *z* axis, so that the intramolecular S···S axes of neighboring TA ions are orthogonal. In the same study it was postulated that "the intermolecular interactions can be easily modulated by electrostatics, crystal packing solvation etc. to produce a variety of polymolecular associates of the same ion radical with parallel or perpendicular, overlapped or laterally shifted monomer orientations." $(TA)_3[Al_2Cl_7]_2$ is now the second compound to feature TA trimers and exhibits the proposed parallel arrangement. The intermolecular S···S distance of neighboring TA molecules of this parallel trimer is much shorter (3.14 Å) than the S···S distance of the crossed trimer (3.98 Å). But due to the shorter interlayer distance, the S···S distance of the two outer TA molecules is smaller in the crossed trimer (6.20 Å) than in the parallel trimer (6.28 Å).

To analyze the differences in the bonding between the parallel and the crossed trimer, we optimized both arrangements in the gas phase as charged, free clusters in the singlet state. The structure optimizations were performed with PBE0-D3 by using the def2-TZVPP basis sets. The parallel trimer, which has C_i symmetry in the bulk, was forced into D_{2h} symmetry, whereas the solid-state structure of the crossed trimer, which already had D_{2h} symmetry, was taken. The calculated total height in the gas phase of the crossed trimer is 6.29 and 6.46 Å for the parallel trimer. For the parallel trimer, the deviation from the experimental value found in the solid is larger than for the crossed trimer, which indicates larger packing effects. Whereas the gas-phase parallel trimer was 14 kJ mol^{-1} lower in energy than the crossed trimer without dispersion interaction, the situation was reversed when the D3 correction was taken into account. At the PBE0-D3 level, the crossed trimer is 2 kJ mol^{-1} more stable than the parallel trimer. Our gas-phase calculations indicate that the dispersion interaction is more attractive (11 kJ mol^{-1}) in the distorted bulk structure in C_i symmetry than in the D_{2h} symmetry. This is apparently the driving force of the observed shifting of the TA molecules in the bulk structure.

In Figure 7 the HOMOs of the charged trimers are shown. In both the crossed and the parallel trimer there is a weak bonding interaction between the orbitals of the outer TA units. The orientation of the central TA molecule does not have a significant effect on the nodal structure of the HOMO, which closely resembles its counterpart in the monomer. The different effect of dispersion in the crossed triple-decker and the parallel trimer must therefore have other reasons and can be tentatively attributed to the different interatomic distances. In a forthcoming paper[36] we will investigate the bonding situation in more detail at a more sophisticated level of theory.

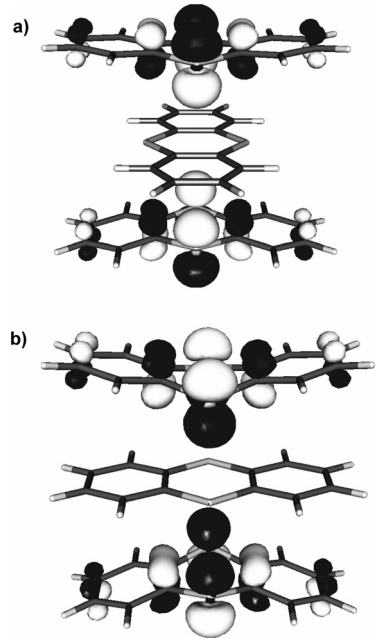

Figure 7. (a) The calculated (PBE0–D3/def2-TZVPP) HOMO of the crossed triple-decker molecule $(TA_3)^{2+}$. (b) The calculated (PBE0–D3/def2-TZVPP) HOMO of the parallel arranged $(TA_3)^{2+}$ trimer in D_{2h} symmetry.

Tris(selenanthrene)aluminum–Tris(heptachloridodialuminate) [Al(SeA)$_3$][Al$_2$Cl$_7$]$_3$

Structure optimizations at PBE and PBE-D2 level were performed for the unit cell in the closed-shell singlet state. The average calculated Se–Al bond length of the cationic complex $[Al(SeA)_3]^{3+}$ is 2.602 Å for PBE and 2.601 Å for PBE-D2, which is in excellent agreement with the experimental value of 2.593 Å. The calculated bending angles α_1, α_2, and α_3 of the coordinating SeA ligands (α_1 is the average of C5–Se2–Se1–C11 and C2–Se1–Se2–C8; for α_2 and α_3 analogously, see Figure 4 and Table 3) are in good agreement with the experiment with maximum deviations of 1.6° for PBE and 1.5° for PBE-D2. The influence of the dispersion correction is low. The band structure was calculated at PBE0 level in the optimized structure (PBE). The calculated band gap at the Γ point is 5.3 eV, thereby classifying $[Al(SeA)_3][Al_2Cl_7]_3$ as a large-band-gap semiconductor, which is in agreement with the observed colorless crystals.

Table 3. Selected calculated structure parameters (lengths in Å, angles in °) of $[Al(SeA)_3][Al_2Cl_7]_3$ and comparison with experimental values. For atom numbering, see Figure 4.

Method	Singlet electronic state		
	Exp.	PBE	PBE-D2
Se–Al7 avg.	2.593(1)	2.602	2.601
α_1 (C–Se–Se–C)	116.8	115.2	115.3
α_2 (C–Se–Se–C)	117.8	117.2	118.4
α_3 (C–Se–Se–C)	119.2	119.0	118.6

Selenanthrene–Tetrachloridoaluminate (SeA)$_2$[AlCl$_4$]$_2$

The primitive unit cell contains four formula units. Structure optimizations at the PBE and PBE-D2 level were per-

formed for the unit cell in the closed-shell singlet and the open-shell nonet state assuming doublet states for all SeA molecules. The singlet state was more stable than the nonet state by 2.9 eV (PBE0 result at the optimized PBE structure). Selected structural parameters of the singlet ground state at PBE and PBE-D2 level are given in Table 4. The results of the structure optimization are in very good agreement with the experiment. The average Se···Se bonds are 3.147 Å for PBE and 3.155 Å for PBE-D. The values of α_1 and α_2 are the dihedral angles C3–Se1–Se2–C9 and C6–Se2–Se1–C12, respectively, which represent the bending of the molecule (see Figure 5). The effect of dispersion on the structure is mainly on the Se radical cation intramolecular bending angles, which is slightly improved by the D2 correction. With each selenanthrene dimer in the triplet state, the average Se···Se and the dihedral angles are larger. The average Se···Se distance is 3.202 Å for PBE and 3.226 Å for PBE-D. The dihedral angles C3–Se1–Se2–C9 are 171.2 (PBE) and 173.8° (PBE-D). The bands of the singlet ground state are rather flat. The calculated band gap at the Γ point is 1.8 eV, thereby classifying $(SeA)_2[AlCl_4]_2$ as a small-band-gap semiconductor.

Table 4. Selected calculated structure parameters (lengths in Å, angles in °) of $(SeA)_2[AlCl_4]_2$ and comparison with experimental values. For atom numbering, see Figure 5.

Method	Singlet electronic state		
	Exp.	PBE	PBE-D2
Se1···Se3	3.1324(2)	3.125	3.113
Se2···Se4	3.1883(2)	3.170	3.197
α_1 (C3–Se1–Se2–C9)	170.34(5)	169.5	171.8
α_2 (C6–Se2–Se1–C12)	172.28(4)	170.8	172.8

Conclusion

The blue to violet colorations that appear over the course of the reaction of thianthrene and neat aluminum chloride are associated with the oxidation of thianthrene to its radical ion. In the solid state, the radicals form trimers $(TA)_3^{2+}$ by association with a neutral molecule and $[Al_2Cl_7]^-$ counterions. TA apparently undergoes an $AlCl_3$-catalyzed redox disproportionation. Under the same conditions, SeA reacts differently and forms the tris-chelate complex $[Al(SeA)_3][Al_2Cl_7]_3$ in a Lewis acid–base reaction. In liquid SO_2 as solvent, TA and SeA show identical reactivity. Both are oxidized to the radical cations, which precipitate out of the solution as dimers $(TA)_2^{2+}$ and $(SeA)_2^{2+}$ with $[AlCl_4]^-$ counterions.

Quantum chemical calculations at the DFT level indicate that the bonding mechanisms in the $(TA)_2^{2+}$ and $(SeA)_2^{2+}$ dimers and in the $(TA)_3^{2+}$ trimers are different. Whereas there is a four-center, two-electron bond between the sulfur and selenium atoms of the dimers, the bonding situation in the trimers is more complex. The crossed trimers are bonded by dispersion forces and the parallel TA trimer features a long-range four-center bond between the outer radicals. In all cases, singlet ground states were found, thus indicating strong coupling between the spin centers. This was confirmed for $(TA)_3[Al_2Cl_7]_2$ by magnetic measurements, which showed a temperature-independent paramagnetism but no signs of free electron spins.

Experimental Section

General Methods: Thianthrene was purchased from Aldrich and first recrystallized from ethanol/toluene and then sublimated under continuous vacuum pumping to remove all traces of water and solvents. Selenanthrene was synthesized from thianthrene *S*,*S*′-dioxide and selenium according to the procedure described.[37] Aluminum chloride was sublimated three times until a pure white material free of traces of $FeCl_3$, which causes a yellowish coloration, was obtained. Commercial SO_2 (product grade 3.8, Praxair) was stored as liquid over P_2O_5 and freshly distilled directly into the reaction vessel prior to use. Additionally, SO_2 was prepared in the following way: P_2O_5 was placed in a round-bottomed flask, and by slow addition of demineralized and degassed water H_3PO_4 was generated. Dry, powdered $NaHSO_3$ was slowly released into the acid with an addition funnel. The released gas was trapped by using an ethanol/dry ice mixture. All operations were performed in a closed, argon-flushed system. The liquefied SO_2 was then treated as described above for the commercial product. Raman spectra were recorded with a Bruker RFS100 FT spectrometer. Magnetic measurements were performed with a Faraday balance on a sample of 1.25 mg included in a quartz capsule by applying five different magnetic fields between approximately 0.1 and 1 T at each temperature point. The data points were corrected for the diamagnetic contribution of the sample container.

Trichloridothianthrene Aluminum(III) and Tris(thianthrenium)–Bis(heptachloridodialuminate): In an argon-filled glovebox, thianthrene (160 mg, 0.74 mmol) and aluminum chloride (100 mg, 0.75 mmol) were placed in a glass ampoule 12 cm in length and 1.2 cm in diameter. The ampoule was evacuated to a final pressure of 1 Pa and flame-sealed. The closed ampoule was first heated at 100 °C for 12 h and then annealed at 50 °C for 3 weeks. The ampoule was opened under a stream of argon and the colorless $\{[AlCl_3(TA)]\}$, dark red $\{(TA)_3[Al_2Cl_7]_2\}$, and yellow crystals that emerged were handled under an inert argon atmosphere.

Tris(selenanthrene)aluminum–Tris(heptachloridodialuminate) $[Al(SeA)_3][Al_2Cl_7]_3$: In an argon-filled glovebox, selenanthrene (100 mg, 0.32 mmol) and $AlCl_3$ (43 mg, 0.32 mmol) were placed in a glass ampoule 14 cm in length and 1.4 cm in diameter. The ampoule was evacuated to a final pressure of 1 Pa and flame-sealed. The closed ampoule was heated at 90 °C for two weeks. The ampoule was opened under a stream of argon and the colorless crystals of $[Al(SeA)_3][Al_2Cl_7]_3$ were isolated in almost quantitative yield and handled under an inert argon atmosphere.

Selenanthrene–Tetrachloridoaluminate: In an argon-filled glovebox, selenanthrene (31 mg, 0.1 mmol) and $AlCl_3$ (27 mg, 0.2 mmol) were placed in an H-shaped vessel. Liquid SO_2 (5 mL) was condensed into each side of the vessel, which resulted in yellow and colorless solutions for selenanthrene and $AlCl_3$, respectively. The solution of $AlCl_3$ was then poured into the solution of selenanthrene. The color of the combined solutions immediately turned dark violet and black crystals with metallic shine started to form after one day. The dark solution was slowly concentrated by distillation of the solvent into the empty branch of the vessel. When the precipitation of white material started, the solution was filtered, thereby leaving behind the black crystals of $(SeA)_2[AlCl_4]_2$ in about 30% yield. $C_{12}H_8AlCl_4Se_2$: calcd. C 30.1, H 1.7; found C 29.0, H 2.1.

X-ray Structure Determinations: Crystals were selected in the glovebox and fixed in glass capillaries, which were sealed by melting. Data collection was performed at low temperature with a Bruker Nonius KappaCCD diffractometer equipped with graphite-monochromated Mo-K_α radiation (λ = 0.71073 Å) and an Oxford Cryostream cooling device. The crystal structures were solved by direct methods and refined using SHELX97.[38] A semiempirical absorption correction by the multiscan method was applied to the data sets.[39] Hydrogen atoms were refined in idealized positions as riding on their attached carbon atoms with isotropic displacement factors fixed to the value 1.2 of the respective C atoms.

CCDC-861629 (for $AlCl_3$(TA)), -861628 (for $(TA)_3[Al_2Cl_7]_2$), -861626 (for $[Al(SeA)_3][Al_2Cl_7]_3$), and -861627 (for $(SeA)_2[AlCl_4]_2$) contain the supplementary crystallographic data for this paper. These data can be obtained free of charge from The Cambridge Crystallographic Data Centre via www.ccdc.cam.ac.uk/data_request/cif.

Trichloridothianthrenealuminum(III) [$AlCl_3$(TA)]: $C_{12}H_8AlCl_3S_2$; triclinic; space group $P\bar{1}$; lattice constants a = 8.1043(2) Å, b = 12.8221(2) Å, c = 14.6312(3) Å, α = 107.234(1)°, β = 93.378(1)°, γ = 91.431(1)°; unit-cell volume 1448.17(5) Å^3; T = 110(2) K; number of formula units Z = 4, $D_{calcd.}$ = 1.604 g cm^{-3}; crystal dimensions 0.10 × 0.10 × 0.08 mm; range of data collection $5.8 \leq 2\theta \leq 55.1°$; range of indices $h \pm 10$, $k \pm 16$, $l \pm 18$; 44591 measured reflections; 6647 unique reflections, R_{merge} = 0.082, absorption coefficient μ = 0.96 mm^{-1}; 325 refined parameters, ratio reflections/parameters: 20.4; reliability factors of refinement $R(|F|)$ for all data: 0.062, $R(|F|)$ for 5000 (F_o) > 4σ(F_o) = 0.036, $wR(F^2)$ = 0.077; max./min. residual density +0.30/–0.39 e Å^{-3}.

Tris(thianthrene)–Bis(heptachloridodialuminate) $(TA)_3[Al_2Cl_7]_2$: $C_{36}H_{24}Al_4Cl_{14}S_6$; monoclinic; space group $P2_1/c$; lattice constants a = 11.3266(3) Å, b = 11.2154(2) Å, c = 22.6814(5) Å, β = 119.896(1)°; unit-cell volume 2497.9(1) Å^3; T = 123(2) K; number of formula units Z = 2, $D_{calcd.}$ = 1.666 g cm^{-3}; crystal dimensions 0.13 × 0.11 × 0.03 mm; range of data collection $6.8 \leq 2\theta \leq 55.1°$; range of indices $h \pm 14$, $k \pm 14$, $l \pm 29$; 21345 measured reflections; 5726 unique reflections, R_{merge} = 0.051, absorption coefficient μ = 1.12 mm^{-1}; 272 refined parameters, ratio reflections/parameters: 21.0; reliability factors of refinement $R(|F|)$ for all data: 0.063, $R(|F|)$ for 4190 (F_o) > 4σ(F_o) = 0.035, $wR(F^2)$ = 0.075; max./min. residual density +0.41/–0.34 e Å^{-3}.

Tris(selenanthrene)aluminum–Tris(heptachloridodialuminate) $[Al(SeA)_3][Al_2Cl_7]_3$: $C_{36}H_{24}Al_7Cl_{21}Se_6$; monoclinic; space group $P2_1/c$; lattice constants a = 13.4410(3) Å, b = 26.9550(4) Å, c = 21.1259(5) Å, β = 122.7232(6)°; unit-cell volume 6439.2(2) Å^3; T = 223(2) K; number of formula units Z = 4, $D_{calcd.}$ = 1.922 g cm^{-3}; crystal dimensions 0.10 × 0.05 × 0.04 mm; range of data collection $3.0 \leq 2\theta \leq 50.8°$; range of indices $h \pm 16$, k –25 to +32, $l \pm 25$; 68672 measured reflections; 11764 unique reflections, R_{merge} = 0.095, absorption coefficient μ = 4.41 mm^{-1}; 631 refined parameters, ratio reflections/parameters: 18.6; reliability factors of refinement $R(|F|)$ for all data: 0.081, $R(|F|)$ for 8160 (F_o) > 4σ(F_o) = 0.042, $wR(F^2)$ = 0.089; max./min. residual density +0.73/–0.71 e Å^{-3}.

Selenanthrene–Tetrachloridoaluminate $(SeA)_2[AlCl_4]_2$: $C_{12}H_8AlCl_4Se_2$; orthorhombic; space group $P2_12_12_1$; lattice constants a = 12.8314(7) Å, b = 13.5237(9) Å, c = 18.3434(11) Å; unit-cell volume 3183.1(3) Å^3; T = 203(2) K; number of formula units Z = 8, $D_{calcd.}$ = 1.999 g cm^{-3}; crystal dimensions 0.27 × 0.09 × 0.04 mm; range of data collection $6.0 \leq 2\theta \leq 54.9°$; range of indices $h \pm 16$, $k \pm 16$, $l \pm 23$; 18320 measured reflections; 6414 unique reflections R_{merge} = 0.111, absorption coefficient μ = 5.35 mm^{-1}; 343 refined parameters, ratio reflections/parameters: 18.7; reliability factors of refinement $R(|F|)$ for all data: 0.112, $R(|F|)$ for 3988 (F_o) > 4σ(F_o) = 0.056, $wR(F^2)$ = 0.124; Flack x parameter 0.001(14), max./min. residual density +0.65/–0.75 e Å^{-3}.

Computational Details: All periodic quantum chemical calculations were performed with the crystalline-orbital program package CRYSTAL09.[27] In CRYSTAL09 the Bloch functions were expanded in atom-centered basis functions. Modified versions[25] of the all-electron basis sets of triple-ζ valence plus polarization (TZVP) quality by Ahlrichs et al.[30,31] were used. For structure optimizations the standard GGA (generalized gradient approximation) functional PBE[23,24] was employed. To study the effect of dispersion interactions on the structures, an empirical correction term proposed by Grimme was applied (PBE-D2).[26]

The hybrid functional PBE0[35] was used for single-point and band-structure calculations. The standard values of CRYSTAL for integral accuracy were increased by a factor of 10 for structure optimizations and by a factor of 100 for single-point calculations. Integration in reciprocal space was performed using a 8 × 8 × 4 Monkhorst–Pack k-point net, which resulted in 90 points in the irreducible Brillouin Zone (IBZ) for $(TA)_3[Al_2Cl_7]_2$, and a 8 × 6 × 4 Monkhorst–Pack k-point net, which resulted in 100 points in the IBZ for $AlCl_3$(TA). For SeA–AlCl4, a 4 × 4 × 4 k-point net with 27 k-points in the IBZ was used.

All gas-phase calculations were carried out with the ORCA program system.[29] The hybrid functional PBE0 with the RIJCOSX approximation[40] in the def2-TPVP basis[30,31] was employed. Figures were generated using Gabedit.[41]

Acknowledgments

The support of this work by the Deutsche Forschungsgemeinschaft (DFG) (German Research Council) within the research framework SFB 813 (Collaborative Research Area) is gratefully acknowledged. We are obliged to Dr. J. Daniels for single crystal selection and data collection, N. Wagner for magnetic measurements, and B. Knopp for experimental assistance.

[1] G. Saito, Y. Yoshida, *Bull. Chem. Soc. Jpn.* **2007**, *80*, 1–137; L. Ouahab, E. Yagubskii (Eds.), *Organic Conductors, Superconductors and Magnets: From Synthesis to Molecular Electronics*, NATO Science Series, Kluwer Academic Publishers, Dordrecht, The Netherlands, **2004**, vol. 139.
[2] J. L. Brusso, O. P. Clements, R. C. Haddon, M. E. Itkis, A. A. Leitch, R. T. Oakley, R. W. Reed, J. F. Richardson, *J. Am. Chem. Soc.* **2004**, *126*, 8256–8265; T. S. Cameron, A. Decken, F. Grein, C. Knapp, J. Passmore, J. M. Rautiainen, K. V. Shuvaev, R. C. Thompson, D. J. Wood, *Inorg. Chem.* **2010**, *49*, 7861–7979.
[3] J. S. Tse, A. A. Leitch, X. Yu, X. Bao, S. Zhang, Q. Liu, C. Jin, R. A. Secco, S. Desgreniers, Y. Ohishi, R. T. Oakley, *J. Am. Chem. Soc.* **2010**, *132*, 4876–4886.
[4] R. S. Glass, *Topics Curr. Chem.* **1999**, *205*, 1–87.
[5] B. K. Bandlish, H. J. Shine, *J. Org. Chem.* **1977**, *42*, 561–563.
[6] H. Bock, A. Rauschenbach, Ch. Näther, M. Kleine, Z. Havlas, *Chem. Ber.* **1994**, *127*, 2043–2049.
[7] J. Beck, T. Bredow, R. T. Tjahjanto, *Z. Naturforsch. B* **2009**, *64*, 145–152.
[8] S. B. Larson, S. H. Simonsen, G. E. Martin, K. Smith, S. Puig-Torres, *Acta Crystallogr., Sect. C* **1984**, *40*, 103–106.
[9] S. V. Rosokha, J. Lu, T. Y. Rosokha, J. K. Kochi, *Acta Crystallogr., Sect. C* **2007**, *63*, o347–o349.
[10] N. W. Alcock, K. P. Ang, K. F. Mok, S. F. Tan, *Acta Crystallogr., Sect. B* **1978**, *34*, 3364–3366.
[11] R. T. Tjahjanto, J. Beck, *Eur. J. Inorg. Chem.* **2009**, 2524–2528.

[12] M. Munakata, S. G. Yan, I. Ino, T. Kuroda-Sowa, M. Maekawa, Y. Suenaga, *Inorg. Chim. Acta* **1998**, *271*, 145–150.
[13] R. T. Tjahjanto, J. Beck, *Z. Naturforsch. B* **2007**, *62*, 1291–1297.
[14] E. A. Meyers, K. J. Irgolic, R. A. Zingaro, T. Junk, R. Chakravorty, N. L. M. Dereu, K. French, G. C. Pappalardo, *Phosphorus Sulfur Silicon Rel. Elem.* **1988**, *38*, 257–269.
[15] K.-W. Stender, G. Klar, D. Knittel, *Z. Naturforsch. B* **1985**, *40*, 774–781.
[16] R. Muller, L. Lamberts, M. Evers, *Electrochim. Acta* **1994**, *39*, 2507–2516.
[17] W. Hinrichs, G. Klar, *J. Chem. Res.* **1982**, *12*, 336–337.
[18] J. M. Hirshon, D. M. Gardner, G. K. Fraenkel, *J. Am. Chem. Soc.* **1953**, *75*, 4115.
[19] H. Bock, U. Lechner-Knoblauch, *J. Organomet. Chem.* **1985**, *294*, 295–304.
[20] W. C. Hodgeman, J. B. Weinrach, D. W. Bennett, *Inorg. Chem.* **1991**, *30*, 1611–1614.
[21] G. Denk, *Fresenius J. Anal. Chem.* **1956**, *153*, 367.
[22] T. Nishinaga, K. Komatsu, *Org. Biomol. Chem.* **2005**, *3*, 561–569.
[23] J. P. Perdew, K. Burke, M. Ernzerhof, *Phys. Rev. Lett.* **1996**, *77*, 3865–3868.
[24] J. P. Perdew, K. Burke, M. Ernzerhof, *Phys. Rev. Lett.* **1997**, *78*, 1396–1396.
[25] M. F. Peintinger, D. Oliveira, T. Bredow, *manuscript in preparation*.
[26] S. Grimme, *J. Comput. Chem.* **2006**, *27*, 1787–1799.
[27] R. Dovesi, V. R. Saunders, R. Roetti, R. Orlando, C. M. Zicovich-Wilson, F. Pascale, B. Civalleri, K. Doll, N. M. Harrison, I. J. Bush, P. D'Arco, M. Llunell, *CRYSTAL09*, User's Manual, University of Torino, Italy, **2009**.
[28] S. Grimme, J. Antony, S. Ehrlich, H. Krieg, *J. Chem. Phys.* **2010**, *132*, 154104.
[29] F. Neese, *The ORCA program system*, Wiley Interdisciplinary Reviews, Computational Molecular Science, **2012**, *2*, pp. 73–78.
[30] A. Schaefer, H. Horn, R. Ahlrichs, *J. Chem. Phys.* **1992**, *97*, 2571–2577.
[31] F. Weigend, R. Ahlrichs, *Phys. Chem. Chem. Phys.* **2005**, *7*, 3297–3305.
[32] M. Lundberg, P. E. M. Siegbahn, *J. Chem. Phys.* **2005**, *122*, 224103.
[33] M. Marsman, J. Paier, A. Stroppa, G. Kresse, *J. Phys. Condens. Matter* **2008**, *20*, 064201.
[34] T. Bredow, A. R. Gerson, *Phys. Rev. B* **2000**, *61*, 5194–5201.
[35] C. Adamo, V. Barone, *J. Chem. Phys.* **1999**, *110*, 6158–6170.
[36] M. F. Peintinger, J. Beck, T. Bredow, manuscript in preparation.
[37] F. Krafft, R. E. Lyons, *Ber. Dtsch. Chem. Ges.* **1896**, *29*, 435–442.
[38] *SHELXS* and *SHELXL*, programs for crystal structure solution and refinement, see: G. M. Sheldrick, *Acta Crystallogr., Sect. A* **2008**, *64*, 112–122.
[39] R. H. Blessing, *Acta Crystallogr., Sect. A* **1995**, *51*, 33–38.
[40] F. Neese, F. Wennmohs, A. Hansen, U. Becker, *Chem. Phys.* **2009**, *356*, 98–109.
[41] *GABEDIT*, a graphical user interface for computational chemistry software, see: A.-R. Allouche, *J. Comput. Chem.* **2011**, *32*, 174–182.

Received: January 22, 2012
Published Online: June 27, 2012

